CONFIDENTIAL: PATENT PENDING

MEASURING BLOOD CELLS VELOCITY IN MICROVESSELS FROM A SINGLE IMAGE: APPLICATION TO *IN VIVO* AND *IN SITU* CONFOCAL MICROSCOPY

N.Savoire[1,2], G. Le Goualher[1], A. Perchant[1], F. Lacombe[1]   *G. Malandain[2], N. Ayache[2]*

[1]Mauna Kea Technologies
9, Rue d'Enghien
75010 Paris, France

[2]EPIDAURE
INRIA
Sophia-Antipolis, Nice, France

ABSTRACT

This article describes an original method to measure the velocity of blood cells in microvessels from a single image. The method exploits a motion artifact produced by laser scanning microscope (LSM). Although velocity can be estimated from a single image, we show how a temporal sequence can then be exploited to increase the robustness and accuracy of the estimation. Preliminary experiments show good quantitative results in synthetic images of microvessels, and good qualitative results with real images of microvessels acquired *in vivo* and *in situ* at a temporal frequency of 12 Hz. A quantitative validation of real measurements is under progress with a specific experimental set-up described in the article.

1. INTRODUCTION

Velocity measurements of blood cells in microvessels are usually obtained from the processing of 2D temporal image sequences obtained in the field of intravital microscopy.
Line shift diagram [1], spatio-temporal analysis [2] or blood cell tracking [3] are used to process temporal sequences generated by CCD-based video microscopes.
Other devices include laser scanning microscopes, where a laser is scanned on the observed tissue sample. Photons reflected by the tissue are then descanned toward a single pixel detector. In such a device a small time interval occurs between each consecutive pixel of the resulting 2D image. Such a scanning is used for the SLO (Scanning Laser Ophtalmoscope) [3] for instance.
We propose to take into account the specificity of laser scanning to obtain velocity information. In particular, we will show that such measurement can be obtained from a single image by taking advantage of motion artifacts induced by moving cells observed using a laser scanning microscope.

2. IMAGE ACQUISITION USING LASER SCANNING DEVICE

2.1. Confocal microscopy

The method proposed in this article to estimate blood cell velocity relies on images acquired through a scanning device. The images presented here are the results of acquisitions made using a Cell-viZio™, a confocal imaging device recently developed by Mauna Kea Technologies[1]. Confocal microscopy allows blur free in depth imaging. Light from out-of-focus regions is rejected by using a pinhole in front of the detector. Confocality can only be assured with point wise imaging, which is why the imaging laser performs a scan to cover the whole field of view. The specificity of Cell-viZio™ is to separate the bulky part which controls the scan (laser and mirrors) and the optical head, and link them by a bundle of fiber optics, allowing *in situ* imaging (e.g. through an endoscope).

2.2. Scanning trajectory

The scanning movement can be decomposed into a fast horizontal sinusoidal component and a slow linear uniform vertical component. Horizontally, the imaging is done only on the central part of the trajectory, where the spot velocity is maximal and nearly constant. Since in this part, the spot horizontal velocity V_x (> 5 m/s) is several orders of magnitude higher than both the spot vertical velocity V_y (~ 2 mm/s) and the velocity V_c of observed Red Blood Cells (RBC) (< 50 mm/s), we make two approximations: the scan lines are horizontal and the time needed by the spot to cross the imaged part is negligible, meaning that the objects are considered motionless during a scan line (which amounts to assuming the horizontal spot velocity infinite).

---

[1]http://www.maunakeatech.com

2.3. Imaging of moving objects

An interesting point of scanning imaging is that the output image is not a representation of a given instant, but a juxtaposition of points corresponding to different moments. Consequently, if there are moving objects in the field of view, what we observe is not the frozen picture of these objects, but the skewed image of these objects because each scan line relates to a different instant, and the objects moved between each scan line. Let us consider a standard 2D+t volume $V(x, y, t)$, without scanning, this volume will be imaged by 2D slices $V(x, y, t_0)$ at different instants t_0. With scanning, the process of image formation comes down to imaging the plane $V(x, y, y/V_y)$ (V_y is the vertical velocity of the scanning). Fig. 1 presents what will be observed when imaging a vertical segment moving horizontally.
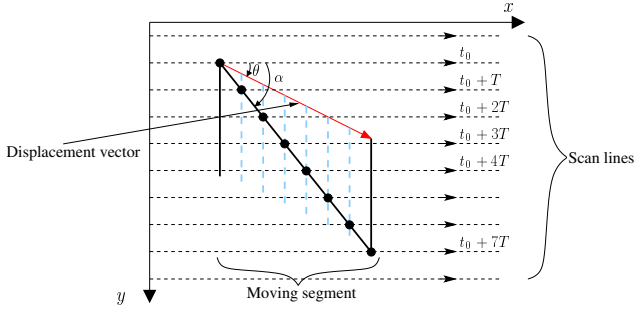

Fig. 1. Imaging of a moving vertical segment by a scanning laser. The segment has a linear movement of angle θ. The segment is first intersected by a scan line at instant t_0 (black disks represent imaged points). The following scan lines image the segment at different positions (dotted segments). The resulting shape is the slanting plain segment of angle α.

3. MODELING OF MOTION INDUCED ARTIFACTS

In this section, we describe the geometric model used to represent RBCs and the deformation of this model induced by the combination of RBC motion and laser scanning.

3.1. RBC model

To understand how RBC images can be distorted by the combination of their own movement and the laser scanning, a very simple model can be used, as shown in figure 1, where RBCs are treated as vertical segments. A much more realistic model would consist in representing RBCs as solid spheres, or even as biconcave surfaces[4], as described in figure 2. In the former case, the orthogonal projection on a plane (which is what we observe) is a disk. In the latter case the projection have no simple analytic form, but can be well approximated by an ellipse, which, for a horizontal

projection plane, degenerates into a disk (Fig. 2). We chose to model RBCs by a disk, this choice will be justified in section 3.3.
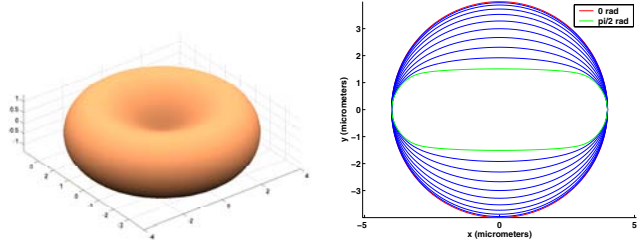

Fig. 2. RBC 3D model (left) and its orthogonal projections on a plane (right).

3.2. Imaging of moving disks

We suppose that a disk of radius R has a linear uniform movement described by a velocity V_c and a trajectory angle θ and is imaged by a scanning laser whose horizontal velocity is infinite and vertical velocity is V_y. The disk will be distorted by the scanning imaging and our goal is to find the equation of the distorted envelope, i.e. the intersection between the disk envelope and the scanning spot.

The points (x_c, y_c) of the envelope of the disk at the instant t verify the equation:

$$\frac{(x_c - V_c t \cos \theta)^2}{R^2} + \frac{(y_c - V_c t \sin \theta)^2}{R^2} = 1 \qquad (1)$$

The vertical position y_s of the spot is given by $y_s = V_y t$. The horizontal spot velocity is supposed infinite, which is why the intersections of the spot trajectory and the envelope are the intersections of the envelope with the line of ordinate y_s. Using $t = y_s/V_y$ in equation 1, we obtain the equation of the distorted envelope:

$$\frac{(x - y V_c \cos \theta/V_y)^2}{R^2} + \frac{(y - y V_c \sin \theta/V_y)^2}{R^2} = 1 \qquad (2)$$

Equation 2 is the equation of an ellipse, i.e. the moving disk will appear as an ellipse in the output image. The angle α (modulo $\pi/2$) of the ellipse axes is given by:

$$\tan 2\alpha = \frac{2 \cos \theta}{V_c/V_y - 2 \sin \theta} \qquad (3)$$

It is this angle α of the ellipses that creates the impression of a dominant orientation in figure 3.

The L length of the major axis is:

$$L = \frac{2R\sqrt{2}}{\sqrt{V_r^2 - 2V_r \sin \theta + 2 - V_r \sqrt{V_r^2 - 4V_r \sin \theta + 4}}} \qquad (4)$$

with $V_r = V_c/V_y$.

Equations 3 and 4 link the velocity and angle θ of the moving disk to the observed values L and α. Given L and α, the inversion of the relations gives two possible solutions for V_c and θ, which implies that only one output image allows to retrieve the velocity and trajectory angle of the disk with an ambiguity between two possibilities. The ambiguity can be removed by considering two scans, one top-down and another bottom-up for example.

One difficulty lies in using L because extracting individual shapes in images like the ones of figure 3 seems unlikely. Only the orientation α can be retrieved, which forbids the use of relation 4. The solution is to suppose the angle of trajectory θ known (for example in image 3, the trajectory of RBCs is supposed colinear to the edges of the vessel). With this hypothesis, the relation 3 allows the determination of the disk velocity.
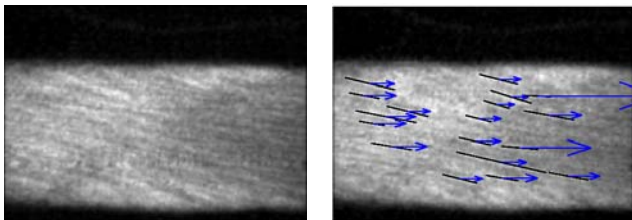

Fig. 3. Mouse cremaster microvessel observed using a Cell-viZio™ (acquisition courtesy of Pr. E. Vicaut). The field of view is about 160x120 microns. Right: example of ridge detection. Slanting segments are the ridge axes. Arrows are the raw velocities estimated from the ridge angles.

3.3. Justification of the disk model

Using a more complex model than the disk to model the projection of an RBC, such as an ellipse, leads to many complications. Contrary to the disk, the ellipse generally has no symmetry of revolution, so the questions which arise are how to set the orientation of the axes and if this orientation remains constant during the movement of the particle. Incidentally the orientation α of the distorted shape depends on this initial orientation.

To overcome these difficulties, we carried out numerical simulations with a realistic bi-concave 3D model[4] (Fig. 2). The protocol was to give the model a random 3D orientation, invariant during the movement, project the shape on the horizontal plane, and measure the orientation of the distorted shape resulting from the scanning. It turns out that the empirical distribution of the angles α presents a sharp peak corresponding to the angle computed for the disk model. Therefore, we conclude that the disk model is sufficient for the retrieval of the velocity information. Additional simulations introducing a random self rotation movement of

the RBCs tend to show that the observed peak remains the same.

4. RIDGE ORIENTATION ESTIMATION

As said before, given figure 3, segmenting individual traces is not possible. In fact, in this sequence, as the plasma is marked by a fluorescent dye, distorted RBC shapes are expected to appear as dark trails. But what we observe seem to be bright trails. Our explanation is that there are so many dark trails that it induces a contrast inversion (given the RBC blood concentration, i.e. 4-5 million per micro-liter of blood, about 1000 RBCs should be in this image) and what we see are the bright interstices between the dark trails. Simulations correlate this explanation (Fig. 4). It is the slope of these white ridges that we want to extract from our images in order to estimate the velocity.

We make the hypotheses that the ridges are elongated, tubular like structures, with a gaussian profile of standard deviation σ_0. Furthermore relation 3 ensures that, for velocities greater than 1 mm/s, the angle α of the ridges is less than $\pi/6$ rad. As a result, we consider that the ridges are almost horizontal. The extraction proceeds in four steps.

First, we enhance the horizontal edges by computing the vertical gradient component $I_y(x, y)$ of the image I. Gradient computation is done by convolving the image with a gaussian kernel derivative with standard deviation σ. This convolution gives two opposite responses per ridge, one for each edge.

Second, since ridges are the points surrounded by a positive response and a negative response at equal distance, we compute a medialness response[5] $R(x, y)$ as such:
$$R(x, y) = I_y(x, y + \sqrt{\sigma_0^2 + \sigma^2}) - I_y(x, y - \sqrt{\sigma_0^2 + \sigma^2})$$
$R(x, y)$ is maximal for the points which belong to ridges. The response $R(x, y)$ is thresholded, with a high threshold, then for each connected region, regional maxima are computed.

Third, the regional maxima are used as seeds to extend the ridges in the horizontal direction. This extension is done by following the maxima of $R(x, y)$ starting from each seed, until a low threshold is reached. This approach is similar to doing a hysteresis thresholding in a privileged direction.

Finally, a line is fitted robustly, using M-estimators, on each extracted ridge to measure the slope. Only ridges whose length are greater than a given threshold, and thus allowing good slope estimation, are kept.

Fig. 3 presents the results of this method. All the extracted ridges may not be valid: a nearly horizontal ridge has been extracted, which gives a huge velocity compared to the other ridges. To make the velocity estimation more robust, it is convenient to consider the ridges of several images and estimate the velocity statistically.

5. EXPERIMENTS

Several experiments have been conducted in order to estimate the correctness of the proposed method.

First a numerical simulator was developed. It models the acquisition of the Cell-viZio™ and simulates a simple laminar flow of RBC (RBC are represented by a 3D model). RBC velocities are randomly set according to normal distribution. Fig 4 presents the resulting images for two RBC concentration. Applying the proposed method and taking the median of the estimated velocities leads to a velocity estimation of $10.57 \, \text{mm/s}$ and $10.25 \, \text{mm/s}$ respectively for the left and right image (the "true" mean velocity is $10 \, \text{mm/s}$).
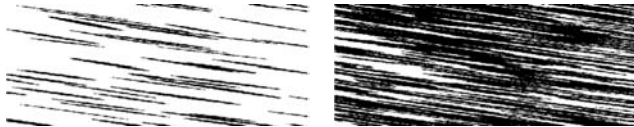

Fig. 4. Simulations of acquisition of 3D RBCs, with 100 cells (left) and 1000 cells (right). The mean velocity was set to $10 \, \text{mm/s}$ and the standard deviation to $1 \, \text{mm/s}$.

Secondly, we applied our method to a sequence of 40 images obtained on real acquisitions of mouse cremaster microvessel. For each image, we computed the median of estimated velocities. Since the actual velocity of RBC in the vessel is unknown, we cannot estimate the correctness of the estimation, nevertheless this enables us to test the stability and robustness of the method. Six images randomly chosen in the sequence with the corresponding median velocity are presented in figure 5. For the whole sequence (40 images), the mean of the median velocity of each image is $7.18 \, \text{mm/s}$ and the standard deviation of the median velocities is $0.7 \, \text{mm/s}$. This result tends to prove that our velocity estimation is stable along the sequence and robust.
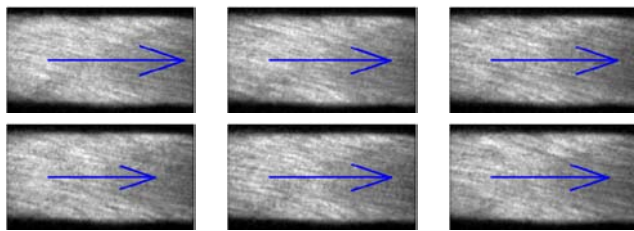

Fig. 5. Median velocities of 6 randomly chosen images from a sequence of 40 images representing real acquisitions on a mouse cremaster microvessel. Mean median velocity is $7.18 \, \text{mm/s}$ and standard deviation of the median velocity is $0.7 \, \text{mm/s}$.

Currently we are building a hydraulic circuit. Water with fluorescent balls whose size is comparable to an RBC

flows in this circuit and the flow velocity is adjustable. This system enables us to compare our velocity estimations with the velocity computed from the rate of flow of the circuit and to validate our method. Fig. 6 presents our first results on a 150 frame sequence (~ 13 seconds) of a uniform linear flow whose velocity is about $21.5 \, \text{mm/s}$ (we do not know yet what is the precision of the velocity computed from the rate of flow). We were able to estimate the flow velocity with a mean relative error of 16%.
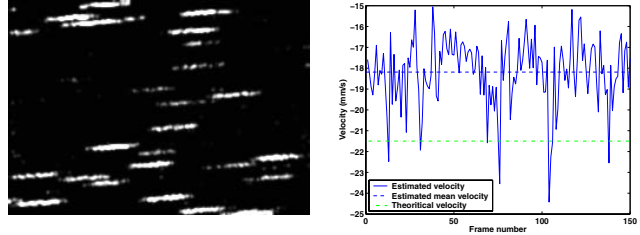

Fig. 6. Results of acquisitions with the hydraulic circuit: Image of moving fluorescent balls (left). Median velocity of each frame of a sequence compared to the actual velocity (right).

6. CONCLUSION

By taking advantage of motion artifacts induced by moving cells observed using a laser scanning microscope, velocity information can be retrieved from a single 2D image. Moreover, as this approach is based on a line scan interaction between the laser scanning and the moving cells, higher velocity can be measured than methods based on analysis of successive temporal frames. When most systems are limited to the measurement of red blood cell velocity inferior to $2 - 5 \, \text{mm/s}$, the presented method allows the measurement of velocities up to $15 - 30 \, \text{mm/s}$.

Work in progress includes use of a hydraulic circuit to model RBCs moving within a microvessel in order to make accurate validation of the proposed method.

7. REFERENCES

[1] K.Messmer editor, *Orthogonal Polarization Spectral Imaging: A new Tool for the Observation and Measurements of the Human Microcirculation*, Karger, 1999.

[2] Y. Sato, J. Chen, R.A. Zoroofi, N. Harada, S. Tamura, and T. Shiga, "Automatic extraction and measurement of leukocyte motion in microvessels using spatiotemporal image analysis," *IEEE Transaction on Biomedical Engineering*, vol. 44, no. 4, pp. 225–236, april 1997.

[3] A Manivannan, Heping Xu, Keith Goatman, Parwez Hossain, Isabel Crane, Peter Sharp Janet Liversidge, and John Forrester, "Cell tracking using SLO angiography," *Ophthalmic Imaging On-Line (http://www.biomed.abdn.ac.uk/Abstracts/A00665/)*, 2002.

[4] Engström KG, "Mechanics of the red blood cell corpuscle: Section modulus, shape, and stringent profile-curvature equation," *J Theor Biol*, vol. 138, pp. 529, 1989.

[5] K. Krissian, G. Malandain, N. Ayache, R. Vaillant, and Y. Trousset, "Model-Based Detection of Tubular Structures in 3D Images," *Computer Vision and Image Understanding*, vol. 80, no. 2, pp. 130–171, 2000.